Quantum spins Hall states in MX_2 (M = Ru, Os; X = As, Sb) monolayers

Tao Jing,[1,*] Dongmei Liang,[1] Yongchen Xiong,[1] Jun Zhang,[1] Yongjin Hu,[1] Qin Zhang,[1] Dongyan Lv,[1] Zhi He,[1] Mingsen Deng,[2,*]

AFFILIATIONS

1 School of Mathematics, Physics and Optoelectronic Engineering, and Collaborative Innovation Center for Optoelectronic Technology, Hubei University of Automotive Technology, Shiyan 442002, People's Republic of China.

2 School of information, Guizhou University of Finance and Economics, Guiyang 550004, People's Republic of China.

Table S1 Lattice parameters of the predicted $RuAs_2$, $RuSb_2$, $OsAs_2$, and $OsSb_2$ monolayers.

	Lattice parameters (Å)		
Phase	1T′	1T	2H
$RuAs_2$	a = 3.062, b = 6.360	$a = b$ = 3.109	$a = b$ = 2.978
	α = 90°	α = 60°	α = 60°
$RuSb_2$	a = 3.273, b = 6.648	$a = b$ = 3.325	$a = b$ = 3.222
	α = 90°	α = 60°	α = 60°
$OsAs_2$	a = 3.093, b = 6.358	$a = b$ = 3.148	$a = b$ = 3.009
	α = 90°	α = 60°	α = 60°
$OsSb_2$	a = 3.285, b = 6.635	$a = b$ = 3.352	$a = b$ = 3.217
	α = 90°	α = 60°	α = 60°

Table S2 Calculated cohesive energies for different phases of MX_2 (M = Ru, Os; X = As, Sb) monolayers.

	$RuAs_2$	$RuSb_2$	$OsAs_2$	$OsSb_2$
1T′	-6.17	-5.70	-6.69	-6.16
2H	-6.16	-5.66	-6.67	-6.09
1T	-6.04	-5.57	-6.53	-6.00

Table S3 Calculated energy oscillation intervals for different MX_2 (M = Ru, Os; X = As, Sb) monolayers after heating at 300K and 500K.

Energy interval (eV)	$RuAs_2$	$RuSb_2$	$OsAs_2$	$OsSb_2$
300K	0.47	0.55	0.54	0.49
500K	0.91	0.70	0.87	0.75

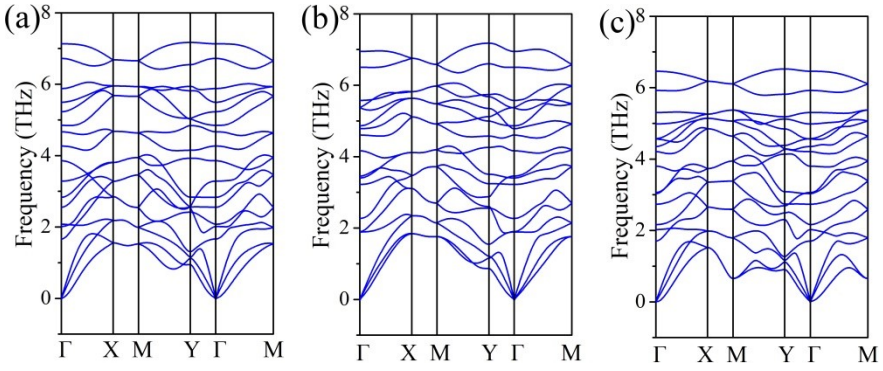

Figure S1 Phonon dispersion of (a) $RuSb_2$, (b) $OsAs_2$, and (c) $OsSb_2$ monolayers, indicating that the structures are dynamically stable.

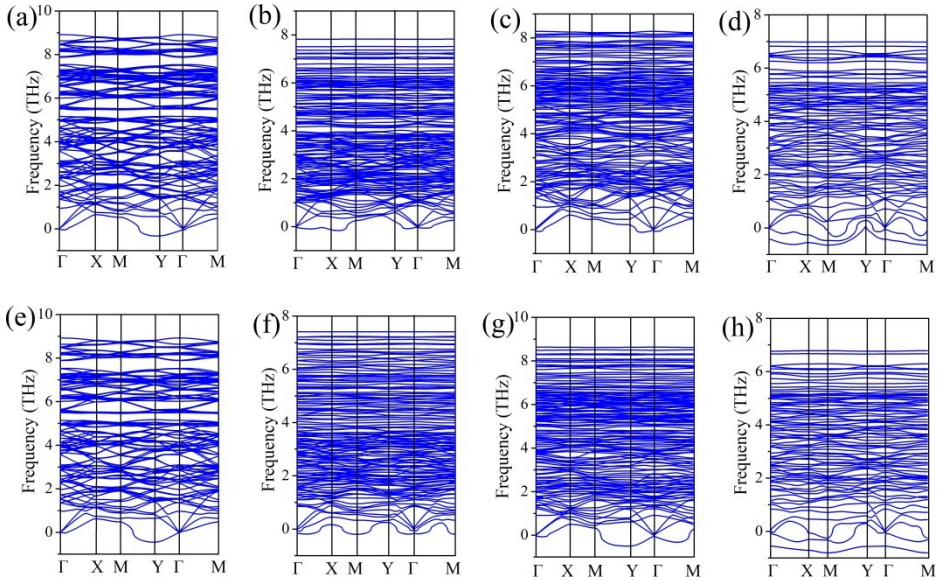

Figure S2 Phonon dispersion of (a) $RuAs_2$, (b) $RuSb_2$, (c) $OsAs_2$, and (d) $OsSb_2$ monolayers after heating at 300K for 5 ps. Phonon dispersion of (e) $RuAs_2$, (f) $RuSb_2$, (g) $OsAs_2$, and (h) $OsSb_2$ monolayers after heating at 500K for 5 ps.

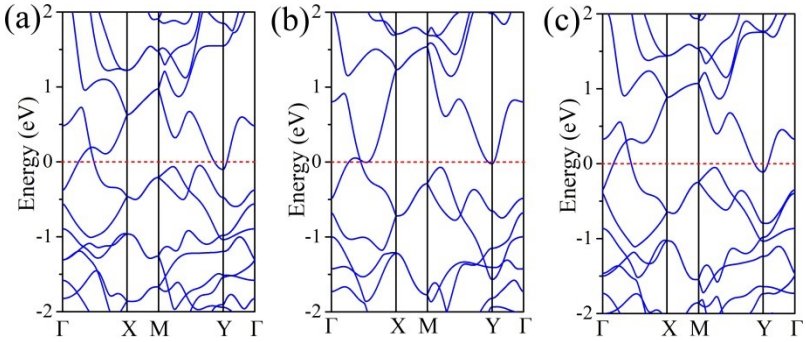

Figure S3 Band structures of (a) $RuSb_2$, (b) $OsAs_2$, and (c) $OsSb_2$ monolayers without SOC.

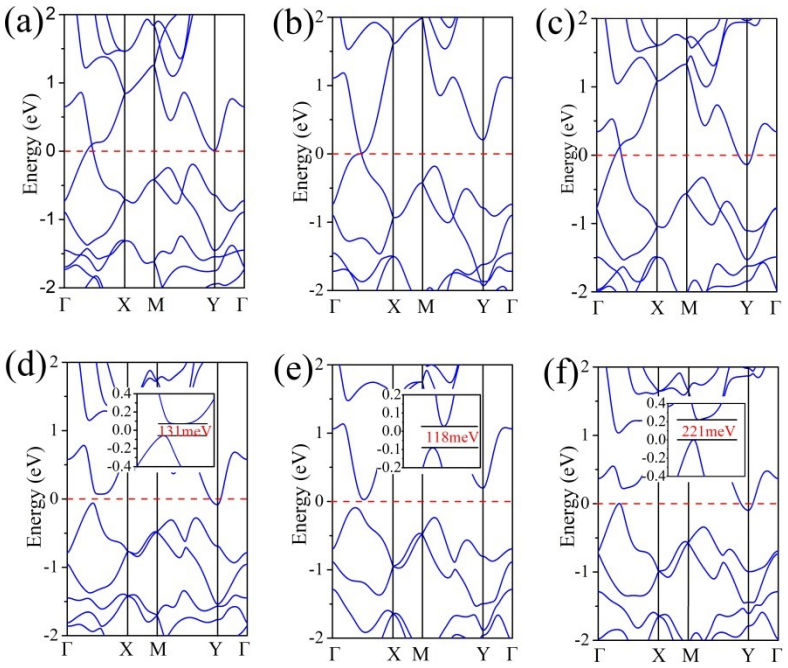

Figure S4 Band structures of (a) $RuSb_2$, (b) $OsAs_2$, and (c) $OsSb_2$ monolayers without SOC. Band structures of (d) $RuSb_2$, (e) $OsAs_2$, and (f) $OsSb_2$ monolayers with SOC. All results are calculated using the hybrid functional (HSE06) method.

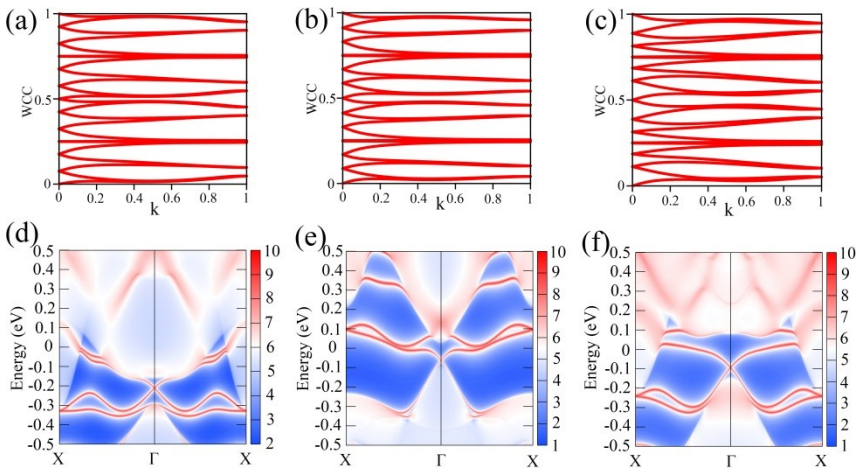

Figure S5 Evolution of the Wannier charge center (WCC) for (a) $RuSb_2$, (b) $OsAs_2$, and (c) $OsSb_2$ monolayers along *k*. Topological edge states of the semi-infinite (d) $RuSb_2$, (e) $OsAs_2$, and (f) $OsSb_2$ monolayers with SOC. All results are calculated using the hybrid functional (HSE06) method.

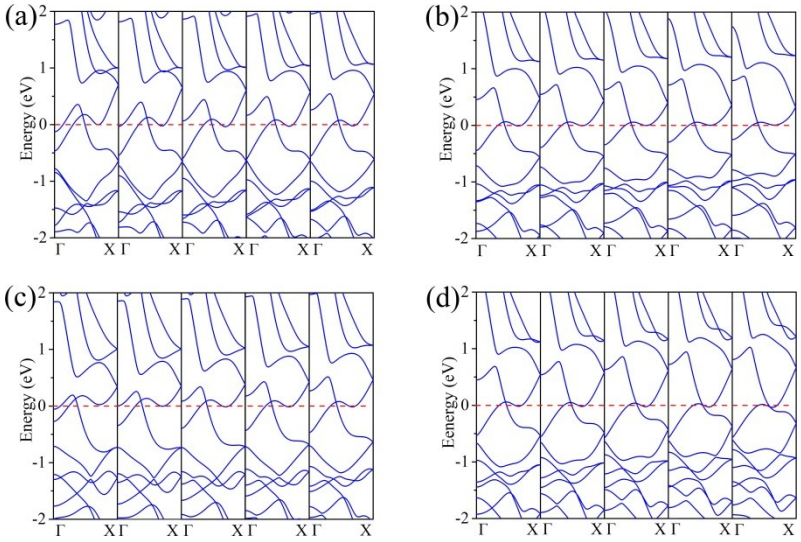

Figure S6 Calculated band structures of $RuSb_2$ monolayers in the strain range from -5% to -1% in the (a) *x* direction and (c) *y* directions, and from 1% to 5% in the (b) *x* direction and (d) *y* directions.

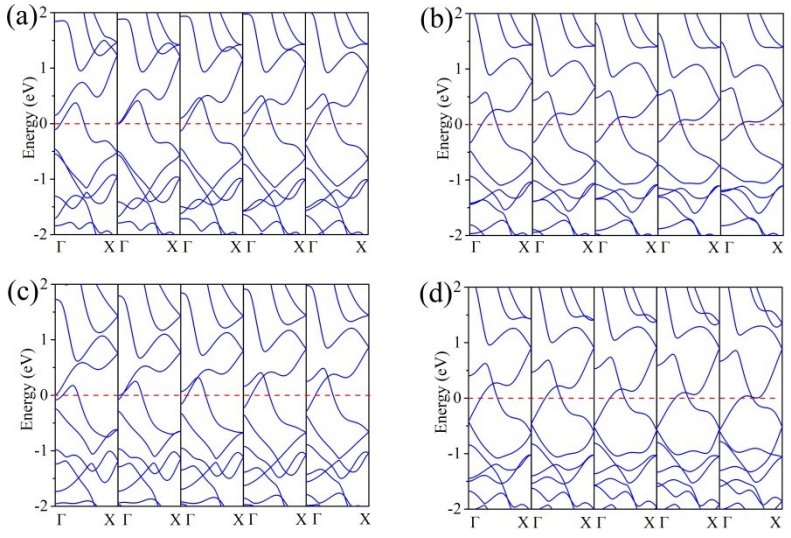

Figure S7 Calculated band structures of $OsSb_2$ monolayers in the strain range from -5% to -1% in the (a) *x* direction and (c) *y* directions, and from 1% to 5% in the (b) *x* direction and (d) *y* directions.